INTERNATIONAL JOURNAL FOR NUMERICAL METHODS IN FLUIDS
Int. J. Numer. Meth. Fluids 2006; **52**:1029–1057
Published online 30 March 2006 in Wiley InterScience (www.interscience.wiley.com). DOI: 10.1002/fld.1220

Flood control of urban stormwater conduit systems using the finite element method

T. Kurahashi*,† and M. Kawahara‡

Department of Civil Engineering, Chuo University, Kasuga 1-13-27 Bukyo-ku, Tokyo 112-8551, Japan

SUMMARY

This paper presents a method of controlling the water levels in a conduit system by employing optimal control theory and the finite element method. A shallow-water equation is employed for the analysis of flow behaviour. Optimal control theory is utilized to obtain a control value for the target state value. The Sakawa–Shindo method is employed as a minimization technique. For the computational storage requirements, the time domain decomposition method is applied. The Crank–Nicolson method is used for temporal discretization. In addition to a method for optimally controlling water level, a method is presented for determining transversality conditions, the terminal condition of the Lagrange multiplier. Copyright © 2006 John Wiley & Sons, Ltd.

KEY WORDS: optimal control theory; finite element method; time domain decomposition method; Sakawa–Shindo method; Lagrange multiplier method; terminal condition for Lagrange multiplier

1. INTRODUCTION

Japan's urban areas continue to expand, due to ceaseless construction of infrastructure, roads, and buildings, leading to a loss of rainfall drainage area and a growing danger of flooding. During heavy rainstorms, existing conduits cannot handle the huge volumes of stormwater that flow directly into them, risking serious flood damage.

In recent years, several kinds of flood control systems have been applied to sewerage systems. One type, which employs existing conduits, has been proposed to guard against flooding. In this study, a water flow distribution system is proposed as a new control system, comprising bypass conduits and control devices. A diagram of this control system is shown

*Correspondence to: T. Kurahashi, Department of Civil Engineering, Chuo University, Kasuga 1-13-27 Bukyo-ku, Tokyo 112-8551, Japan.
†E-mail: tkura@civil.chuo-u.ac.jp
‡E-mail: kawa@civil.chuo-u.ac.jp

Received 1 November 2005
Revised 31 January 2006
Accepted 5 February 2006

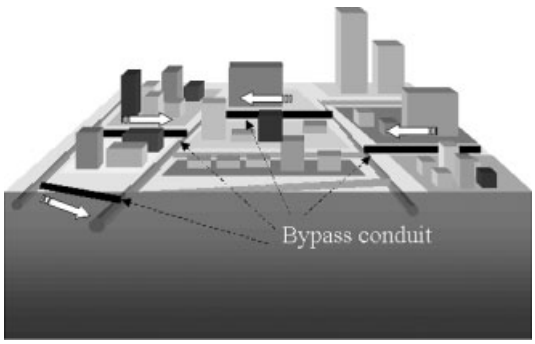

Figure 1. Diagram of flood control system (I).

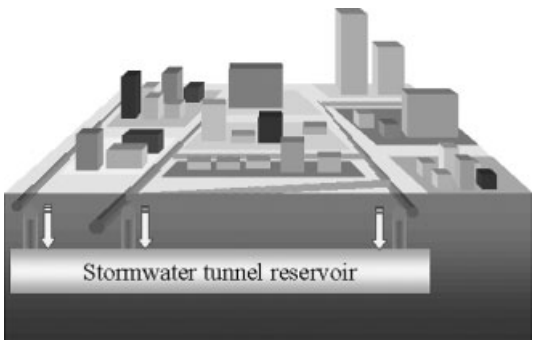

Figure 2. Diagram of flooding control system (II).

in Figure 1. This control system is usable if existing conduits have space which can be used to store stormwater when a storm occurs.

On the other hand, as a traditional countermeasure of flooding, stormwater tunnel reservoirs are constructed to reduce flooding damage. However, it has recently been reported that this strategy does not function effectively. There are several problems with the side weirs that act passively as intake structures. It has been proposed that side weirs operated by an administrator or automatically, and that, in this flooding control system, the stormwater should be injected in a planned way into stormwater tunnel reservoirs using a control device. A diagram of this control system is shown in Figure 2.

In this study, numerical examples, multi-conduit problems and complicated conduit networks are used to confirm the efficacy of these control systems, with the aim of obtaining optimal control discharge to reduce water level to a target value. The technique used is optimal control theory, a methodology for obtaining optimal design variables by using adjoint equations. It is commonly used when design parameters shape need to determined References [1, 2].

In this study, we assume that the water flowing in the conduit has, an exposed surface, allowing the water flow to described in terms of shallow water flow. Concerning the flow into side weirs, it has been reported that flow behaviour can be precisely expressed using

a two-dimensional shallow-water equation [3], and thus we have used this technique to express flow behaviour in this study.

Concerning the optimization problem, the treatment of the transversality condition (the terminal condition of Lagrange multiplier) is important in evaluating the control value at the terminal time. Conventionally, the terminal condition of the Lagrange multiplier has been treated as zero [4]. However, since this approach is not always satisfactory, in this paper we propose a method by which the distribution of the Lagrange multiplier is determined at the terminal time.

2. STATE EQUATION

Using the indicial notation and summation convention, the shallow-water equation is employed to calculate the flow behaviour, which is as follows:

$$\dot{u}_i + u_j u_{i,j} + g\eta_{,i} - \nu(u_{i,j} + u_{j,i})_{,j} + f u_i = 0 \quad \text{in } \Omega \tag{1}$$

$$\dot{\eta} + \{(h+\eta)u_i\}_{,i} = 0 \quad \text{in } \Omega \tag{2}$$

u_i denotes water velocity, η represents the water elevation, g is acceleration due to gravity and h is water depth. Kinematic eddy viscosity is expressed by ν, which is expressed as

$$\nu = \frac{\kappa_l}{6} u_* h$$

where κ_l is the Kalman constant and u_* is velocity of friction which is given as

$$u_* = \frac{g n^2 u_k^2}{h^{1/3}}$$

and f, the bottom of friction term, can be denoted as

$$f = \frac{g n^2}{(h+\eta)^{4/3}} \sqrt{u_k u_k}$$

where n is Manning's roughness coefficient.

Computational domain and boundaries are described in Figure 3.

Here, the boundary conditions of the shallow-water equation are defined as follows:

$$u_i = \hat{u_i} = (\hat{u}, 0), \quad \eta = \hat{\eta} \quad \text{on } \Gamma_U \tag{3}$$

$$t_i = (0,0) \quad \text{on } \Gamma_D \tag{4}$$

$$t_x = 0, \quad v = 0 \quad \text{on } \Gamma_S \tag{5}$$

$$u_i = \bar{u_i} = (0, \bar{v}) \quad \text{on } \Gamma_{\text{con}} \tag{6}$$

where t_i is traction, and is given as,

$$t_i = \nu(u_{i,j} + u_{j,i}) n_j = \hat{t}_i \quad \text{on } \Gamma_S \tag{7}$$

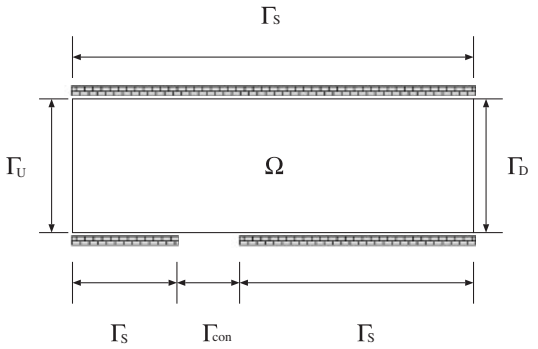

Figure 3. Computational domain and boundary conditions.

In addition, Γ_U means the inflow boundary, Γ_D means the outflow boundary, Γ_S means the wall boundary and Γ_{con} means the boundary that the control discharge is given. If the boundary Γ_S is a curved line, water velocities u_i, are denoted as,

$$u_n = u_i n_i = \hat{u}_n \quad \text{on } \Gamma_S \tag{8}$$

where n_i denotes the direction cosine of the unit outward normal of the boundary. The overhat $\hat{}$ expresses the given value on the boundary.

The initial conditions are given as follows:

$$u_i = \hat{u}_{i0} \quad \text{in } \Omega \quad \text{at } t = t_0 \tag{9}$$

$$\eta = \hat{\eta}_0 \quad \text{in } \Omega \quad \text{at } t = t_0 \tag{10}$$

2.1. Discretization in space

For the spatial discretization of the shallow-water equation, the Galerkin method using the bubble function element with the stabilization parameter is applied. This method is very useful for the problem that the water surface is discontinuous. In case that the water surface is discontinuous, the shock wave occurs at the top and bottom points of the discontinuous water surface. To control the shock wave, the Galerkin method using the bubble function element with the stabilization parameter is very useful. Therefore, this method is employed to analyse the shallow-water flow. Bubble function interpolation is applied as the interpolation function for the weighting function and state variables. The interpolation function for velocities and water elevation can be expressed as

$$u_i = \Phi_1 u_{i1} + \Phi_2 u_{i2} + \Phi_3 u_{i3} + \Phi_4 \tilde{u}_{i4} \tag{11}$$

$$\eta = \Phi_1 \eta_1 + \Phi_2 \eta_2 + \Phi_3 \eta_3 + \Phi_4 \tilde{\eta}_4 \tag{12}$$

As for the interpolation function of the weighting function, the same type of interpolation function is employed. State variables at the gravity points at each element, $\tilde{u}_{i4}$ and $\tilde{\eta}_4$, are written as

$$\tilde{u}_{i4} = u_{i4} - \tfrac{1}{3}(u_{i1} + u_{i2} + u_{i3}) \tag{13}$$

$$\tilde{\eta}_4 = \eta_4 - \tfrac{1}{3}(\eta_1 + \eta_2 + \eta_3) \tag{14}$$

The shape function, which is C^0 continuous can be defined as

$$\Phi_1 = N_1, \quad \Phi_2 = N_2, \quad \Phi_3 = N_3 \tag{15}$$

$$\Phi_4 = 27 N_1 N_2 N_3 \tag{16}$$

where N_1–N_3 are linear interpolation function.

By applying the bubble function interpolation for the weighted residual equations which can be obtained by the Galerkin method, the finite element equation can be obtained as

$$M\dot{u}_i + S_j(u_j^{\text{adv}})u_i + gS_i\eta + v(H_{jj}u_i + H_{ji}u_j) + fMu_i = T_i \tag{17}$$

$$M\dot{\eta} + S_i(u_i^{\text{adv}})h + S_i(u_i^{\text{adv}})\eta + S_i((h+\eta)^{\text{adv}})u_i = 0 \tag{18}$$

where matrices M, $S_i((u_i^{\text{adv}}))$, $S_j(u_j^{\text{adv}})$, $S_i((h+\eta)^{\text{adv}})$, H_{ii}, H_{ji} and H_{jj} denote the coefficients of the finite element equations. The traction vector for water velocities is denoted by T_i. u_i^{adv} and $(h+\eta)^{\text{adv}}$ mean the advection variables for the non-linear terms.

2.2. Discretization in time

For the temporal discretization of the finite element equations, the Crank–Nicolson method is applied. This method is well known as the scheme that it is possible to compute stably. The finite element equations discretized in the temporal direction can be obtained as

$$M\frac{u_i^{n+1} - u_i^n}{\Delta t} + S_j(u_j^{\text{adv}})u_i^{n+(1/2)} + gS_i\eta^{n+(1/2)} + v(H_{jj}u_i^{n+(1/2)} + H_{ji}u_j^{n+(1/2)}) + fMu_i^{n+(1/2)} = T_i^n \quad \text{in } \Omega \tag{19}$$

$$M\frac{\eta^{n+1} - \eta^n}{\Delta t} + S_i(u_i^{\text{adv}})h^{n+(1/2)} + S_i(u_i^{\text{adv}})\eta^{n+(1/2)} + S_i((h+\eta)^{\text{adv}})u_i^{n+(1/2)} = 0 \quad \text{in } \Omega \tag{20}$$

where $u_i^{n+(1/2)}$, $h^{n+(1/2)}$, $\eta^{n+(1/2)}$, advection velocity u_i^{adv} and $(h+\eta)^{\text{adv}}$ are expressed as

$$u_i^{n+(1/2)} = \tfrac{1}{2}(u_i^{n+1} + u_i^n), \quad h^{n+(1/2)} = \tfrac{1}{2}(h^{n+1} + h^n) = h, \quad \eta^{n+(1/2)} = \tfrac{1}{2}(\eta^{n+1} + \eta^n) \tag{21}$$

$$u_i^{\text{adv}} = \tfrac{1}{2}(3u_i^n - u_i^{n-1}), \quad (h+\eta)^{\text{adv}} = \tfrac{1}{2}(3(h+\eta)^n - (h+\eta)^{n-1}) = h + \tfrac{1}{2}(3\eta^n - \eta^{n-1}) \tag{22}$$

u_i^{adv} and $(h+\eta)^{\text{adv}}$ are quasi-linear approximations of advection velocity, given by the Adams–Bashforth formula, and have second-order accuracy. Therefore, in the temporal direction, this discretization is the linear scheme which has second-order accuracy.

2.3. Derivation of stabilized operator control term for bubble function

A stabilization parameter has to be included in the finite element equation if the bubble function element is used. Therefore, a stabilization parameter is introduced to add numerical viscosity [5, 6]. The bubble function is able to eliminate the barycentre point using static condensation. If static condensation is applied to the bubble function, the stabilization parameter derived by the bubble function is equivalent to that derived by formulation of the SUPG method (streamline-upwind/Petrov–Galerkin method [7]). The stabilization parameters for the shallow-water equation discretized by the Galerkin method using the bubble function element can be derived as follows.

2.3.1. Stabilization parameters for bubble function. For the momentum equation and the continuity equation, the stabilization parameters for bubble function can be obtained as

$$\tau_{eBu_i} = \frac{\langle \phi_e, 1 \rangle^2_{\Omega_e} A_e^{-1}}{(1/\Delta t)\|\phi_e\|^2_{\Omega_e} + \frac{1}{2}[(v+v')2\|\phi_{e,j}\|^2_{\Omega_e} + f\|\phi_e\|^2_{\Omega_e}]} \tag{23}$$

$$\tau_{eB\eta} = \frac{\langle \phi_e, 1 \rangle^2_{\Omega_e} A_e^{-1}}{(1/\Delta t)\|\phi_e\|^2_{\Omega_e} + \frac{1}{2}[(v')\|\phi_{e,i}\|^2_{\Omega_e}]} \tag{24}$$

where v' is a control parameter for the stable operation. This parameter can be determined such that this value is equivalent to the following parameters derived by the SUPG method.

2.3.2. Stabilization parameters derived by SUPG method. For the momentum equation and the continuity equation, the stabilization parameters derived by the SUPG method can be written as

$$\tau_{eBu_i} = \left(\frac{1}{2}\tau^{-1}_{eSu_i} + \frac{\alpha}{\Delta t} \right)^{-1} \tag{25}$$

$$\tau_{eB\eta} = \left(\frac{1}{2}\tau^{-1}_{eS\eta} + \frac{\alpha}{\Delta t} \right)^{-1} \tag{26}$$

where $\tau^{-1}_{eSu_i}$, $\tau^{-1}_{eS\eta}$ and α are calculated as

$$\tau^{-1}_{eSu_i} = \left[\left(\frac{2|U_{si}|}{h_e} \right)^2 + \left(\frac{4v}{h_e^2} \right)^2 \right]^{1/2}, \quad \tau^{-1}_{eS\eta} = \frac{2|U_{si}|}{h_e}, \quad \alpha = \frac{A_e||\phi_e||^2_{\Omega_e}}{\langle \phi_e, 1 \rangle_{\Omega_e}} \tag{27}$$

Finally, at the gravity points for each element, the stabilized operator control term can be obtained as follows.

2.3.3. Stabilized operator control terms at gravity points for each element. Those terms for the momentum equation and the continuity equation can be shown as

$$(v+v')2\|\phi_{e,j}\|^2_{\Omega_e} = \frac{\langle \phi_e, 1 \rangle^2_{\Omega_e}}{A_e}\tau^{-1}_{eSu_i} - f||\phi_e||^2_{\Omega_e} \tag{28}$$

The term for continuity equation can then be shown as

$$v'\|\phi_{e,i}\|^2_{\Omega_e} = \frac{\langle \phi_e, 1\rangle^2_{\Omega_e}}{A_e}\tau^{-1}_{eS\eta} \tag{29}$$

Here, these terms can be operated as the numerical viscosity at the gravity points of each element. The role of these terms is to control the numerical oscillation. In addition, $|U_{si}|$, h_e, $\langle \phi_e, 1\rangle_{\Omega_e}$ and $\|\phi_e\|^2_{\Omega_e}$ are written as

$$|U_{si}| = \sqrt{u^2 + v^2 + gh} \tag{30}$$

$$h_e = \sqrt{2A_e} \tag{31}$$

$$\langle \phi_e, 1\rangle_{\Omega_e} = \frac{A_e}{3} \tag{32}$$

$$\|\phi_e\|^2_{\Omega_e} = \frac{A_e}{6} \tag{33}$$

where A_e means the area of an element. A_e is calculated as $\int_{\Omega_e} \mathrm{d}\Omega$.

3. OPTIMAL CONTROL THEORY

3.1. Definition of performance function

Optimal control theory is employed to obtain the control value for the target state. The performance function is expressed as the square sum of the residual between the computed and target water levels, the square form of the control water velocity and the square sum of the residual between the computed and target water levels at the terminal time. The performance function is expressed as

$$J = \frac{1}{2}\int_{t_0}^{t_f}\int_{\Omega}(\eta - \eta_{\mathrm{Target}})^{\mathrm{T}} Q(\eta - \eta_{\mathrm{Target}})\,\mathrm{d}\Omega\,\mathrm{d}t + \frac{1}{2}\int_{t_0}^{t_f}\int_{\Omega}\bar{u}_i^{\mathrm{T}} R\bar{u}_i\,\mathrm{d}\Omega\,\mathrm{d}t$$
$$+ \frac{1}{2}\int_{t_0}^{t_f}\int_{\Omega}(\eta(t_f) - \eta_{\mathrm{Target}}(t_f))^{\mathrm{T}} W(\eta(t_f) - \eta_{\mathrm{Target}}(t_f))\,\mathrm{d}\Omega\,\mathrm{d}t \tag{34}$$

where Q, R and W are weighting constants, η is the computed water level and η_{Target} is the target water level and $\bar{u}_i$ denotes optimal control velocity. The weighting constants Q, R and W mean the values which are set to take a balance of the computed value for each terms of the performance function. For instance, if we can ignore the scale of the control device, we can set $Q = 1.0$, $R = 0.0$ and $W = \hat{W}$. In addition, if we would like to precisely express the control value near the terminal time, we can set the weighting constant W based on the value of weighting constant Q. The set of the weighting constants depends on the each control problems. Therefore, according to the problem, the weighting constants should be appropriately set. Here, the purpose of this study is to find the optimal control discharge $\bar{Q}$ which is calculated by $\bar{u}_i$ to minimize the performance function under the constraints of the shallow-water equation, initial conditions and boundary condition. Minimizing the performance

function means that the computed water level should be as close as possible to the target water level. Here, the target water level is a pre-assigned value that is predicted not to cause any flooding. To determine the distribution of the Lagrange multiplier at the terminal time, the last term of the performance function is added.

3.2. Derivation of adjoint equation

The performance function is constrained by the state equation. The Lagrange multiplier method is applicable to minimizing the performance function with constraint conditions. The extended performance function is therefore introduced using the Lagrange multiplier, multiplied by the state equation. As the state equation which is added to the performance function, discretized finite element equations in the spatial direction are employed. The extended performance function is expressed as follows:

$$J^* = J + \int_{t_0}^{t_f}\int_{\Omega} (L - u_i^{*\mathrm{T}} M\dot{u}_i - \eta^{*\mathrm{T}} M\dot{\eta}) \tag{35}$$

where u_i^* and η^*, respectively, denote the Lagrange multipliers for water velocity and water elevation. Scalar value L is expressed as

$$\begin{aligned} L = {} & u_i^{*\mathrm{T}}(-S_j(u_j^{\mathrm{adv}})u_i - gS_i\eta - \nu(H_{jj}(\nu')u_i + H_{ji}(\nu')u_j) - fMu_i - T_i) \\ & + \eta^{*\mathrm{T}}(-S_i(u_i^{\mathrm{adv}})h - S_i(u_i^{\mathrm{adv}})\eta - S_i((h+\eta)^{\mathrm{adv}})u_i + A(\nu')\eta) \end{aligned} \tag{36}$$

where matrices M, $S_i((u_i^{\mathrm{adv}}))$, $S_j(u_i^{\mathrm{adv}})$, $S_i((h+\eta)^{\mathrm{adv}})$, $H_{ji}(\nu')$, $H_{jj}(\nu')$ and $A(\nu')$ denote the coefficients derived by the Galerkin method using the bubble function element with stabilized operator control term and T_i means the traction vector for water velocity. In addition, the scalar value L means the terms that the steady terms for the discretized state equation (17) and (18), are multiplied by the Lagrange multipliers. As the necessary condition under which J^* should be stationary, the first variation of J^* must be zero, which is calculated as

$$\begin{aligned} \delta J^* = {} & \int_{t_0}^{t_f}\int_{\Omega} \left\{ \delta u_i^{*\mathrm{T}} \left(\frac{\partial L}{\partial u_i^*} - M\dot{u}_i \right) + \delta\eta^{*\mathrm{T}} \left(\frac{\partial L}{\partial \eta^*} - M\dot{\eta} \right) \right. \\ & + \left(\frac{\partial L}{\partial u_i}^{\mathrm{T}} + \dot{u}_i^{*\mathrm{T}} M \right) \delta u_i + \left(\frac{\partial L}{\partial \eta}^{\mathrm{T}} + \dot{\eta}^{*\mathrm{T}} M + (\eta - \eta_{\mathrm{Target}})^{\mathrm{T}} Q \right) \delta\eta \\ & \left. + \left(\frac{\partial L}{\partial \bar{u}_i}^{\mathrm{T}} + \dot{u}_i^{*\mathrm{T}} M + \bar{u}_i{}^{\mathrm{T}} R \right) \delta\bar{u}_i \right\} \mathrm{d}\Omega\,\mathrm{d}t + \int_{t_0}^{t_f}\int_{\Omega} \left\{ \left(\frac{\partial L}{\partial u_i(t_f)}^{\mathrm{T}} \right) \delta u_i(t_f) \right. \\ & \left. + \left(\frac{\partial L}{\partial \eta(t_f)}^{\mathrm{T}} + (\eta(t_f) - \eta_{\mathrm{Target}}(t_f))^{\mathrm{T}} W \right) \delta\eta(t_f) \right\} \mathrm{d}\Omega\,\mathrm{d}t \\ & - \int_{\Omega} \{ u_i^{*\mathrm{T}}(t_0) M\delta u_i(t_0) - u_i^{*\mathrm{T}}(t_f) M\delta u_i(t_f) \\ & + \eta^{*\mathrm{T}}(t_0) M\delta\eta(t_0) - \eta^{*\mathrm{T}}(t_f) M\delta\eta(t_f) \}\, \mathrm{d}\Omega \end{aligned} \tag{37}$$

Therefore, the adjoint equations for the Lagrange multipliers can be obtained in the following form:

$$M^{\mathrm{T}}\dot{u}_i^* + \frac{\partial L}{\partial u_i} = T_i^* \quad \text{in } \Omega \tag{38}$$

$$M^{\mathrm{T}}\dot{\eta}^* + \frac{\partial L}{\partial \eta} + Q^{\mathrm{T}}(\eta - \eta_{\mathrm{Target}}) = 0 \quad \text{in } \Omega \tag{39}$$

Here, the boundary conditions for the Lagrange multipliers are defined as follows:

$$u_i{}^* = (0,0), \quad \eta^* = 0 \quad \text{on } \Gamma_U \tag{40}$$

$$t_i^* = (0,0) \quad \text{on } \Gamma_D \tag{41}$$

$$t_x^* = 0, \quad v^* = 0 \quad \text{on } \Gamma_S \tag{42}$$

$$u_i{}^* = (0,0) \quad \text{on } \Gamma_{\mathrm{con}} \tag{43}$$

where t_i^* means the traction vector for Lagrange multipliers. As well as the case of the state equation, Γ_U means the inflow boundary, Γ_D means the outflow boundary, Γ_S means the wall boundary and Γ_{con} means the boundary that the control discharge is given.

In addition, the gradient of performance function with respect to control velocity can be obtained as

$$\frac{\partial J^*}{\partial \bar{u}_i} = t_i^* = \frac{\partial L}{\partial \bar{u}_i}^{\mathrm{T}} + \dot{u}_i^{*\mathrm{T}} M + \bar{u}_i{}^{\mathrm{T}} R \tag{44}$$

In this paper, a method for determining the distribution of the terminal condition over the whole domain is proposed. If the adjoint equation is solved, it is necessary to determine the terminal condition of the Lagrange multipliers. Conventionally, the terminal condition of the Lagrange multiplier has been treated as zero in all iteration cycles.

If the distribution of the terminal condition is expressed by a steady adjoint equation, the terminal condition is determined by solving the following equations:

$$\frac{\partial L}{\partial u_i(t_f)} = T_i^* \quad \text{in } \Omega \quad \text{at } t = t_f \tag{45}$$

$$\frac{\partial L}{\partial \eta(t_f)} + W^{\mathrm{T}}(\eta(t_f) - \eta_{\mathrm{Target}}(t_f)) = 0 \quad \text{in } \Omega \quad \text{at } t = t_f \tag{46}$$

Finally, if the performance function is converged, the water level at the terminal time approaches the target water level η_{Target}. Therefore, at the final iteration, the solution of the above equation arrives at zero, meaning that the terminal condition of the Lagrange multiplier becomes zero at the final iteration. Consequently, the necessary condition for which the extended performance function is stationary is satisfied at the final iteration. For the temporal discretization of the adjoint equation, the Crank–Nicolson method is applied.

4. MINIMIZATION TECHNIQUE

4.1. The Sakawa–Shindo method

The Sakawa–Shindo method is applied as the minimization technique [8]. In this method, a modified performance function to which a penalty term is added is introduced. The modified performance function is written as

$$K = J^{*(l)} + \frac{1}{2}\int_{t_0}^{t_f}\int_{\Omega} (\bar{u_i}^{(l+1)} - \bar{u_i}^{(l)})^{\mathrm{T}} W^{(l)} (\bar{u_i}^{(l+1)} - \bar{u_i}^{(l)})\,\mathrm{d}\Omega\,\mathrm{d}t \tag{47}$$

where l is the iteration number for the minimization, $\bar{u}_i$ is the control water velocity and $W^{(l)}$ is the weighting parameter. By applying the stationary condition, $\delta K = 0$, the following equation can be obtained. The optimal control water velocity is renewed by the following equation:

$$W^{(l)\mathrm{T}} \bar{u_i}^{(l+1)} = W^{(l)\mathrm{T}} \bar{u_i}^{(l)} - \frac{\partial J^{*(l)}}{\partial \bar{u_i}} \quad \text{on } \Gamma_{\mathrm{con}} \tag{48}$$

where Γ_{con} means the control boundary. Finally, the control discharge $\bar{Q}$ can be calculated as

$$\bar{Q} = \int_{\Gamma_{\mathrm{con}}} (h + \eta)|\bar{U}_i|\,\mathrm{d}\Gamma \tag{49}$$

where $|\bar{U}_i|$ is calculated as

$$|\bar{U}_i| = \sqrt{\bar{u}^2 + \bar{v}^2} \tag{50}$$

The algorithm of the Sakawa–Shindo method is shown below.

1. Choose an initial control value, $\bar{u_i}^{(l)}$.
2. Compute $u_i^{(l)}$ and $\eta^{(l)}$ using the state equation and the initial performance function $J^{(l)}$.
3. Compute $u_i^{*(l)}$ and $\eta^{*(l)}$ using the adjoint equation.
4. Generate a new control value $\bar{u_i}^{(l+1)}$ using Equation (48).
5. Check for convergence; if $\|\bar{u_i}^{(l+1)} - \bar{u_i}^{(l)}\| < \varepsilon$ then stop or go to step 6.
6. Compute $u_i^{(l+1)}$ and $\eta^{(l+1)}$ using the state equation and the performance function $J^{(l+1)}$.
7. Renew the weighting parameter $W^{(l)}$; if $J^{(l+1)} \leqslant J^{(l)}$, then set $W^{(l+1)} = 0.9W^{(l)}$ and go to step 3 else set $W^{(l+1)} = 2.0W^{(l)}$ and go to step 4.

4.2. Time domain decomposition method

In principle, solution of the state equation at all discretization points in space and time is required to solve the adjoint equation. For large-scale optimization problems, numerous computational storage requirements are required, making it almost impossible to store the solutions of the state equation at all time discretization points. Thus, a method that can drastically reduce storage requirements is needed, and is described below. The time domain decomposition method (TDDM) is employed as a technique for reducing the storage requirement

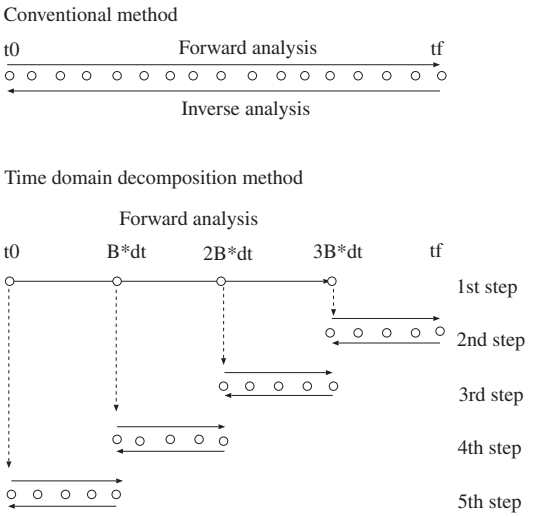

Figure 4. Subdivision of $[0, t_f]$, $A = 5$, $B = 5$, $N = 25$.

[9, 10]. The algorithm or the TDDM can be described as follows:

1. Assume the number of time steps to be N.
2. Consider positive integers A and B; the meanings of A and B are the number of divisions and the number of time steps in the divided section, such that $AB = N$.
3. Decompose the interval [0, t_f] in A subintervals of length $B\Delta t$.
4. Solve the state equation and store the solution for $n = iB$ and $i = 0, 1, \ldots, A-1$, and then for $n = (A-1)B + j$ and $j = 1, 2, \ldots, B$, which are shown in Figure 4.
5. Solve the adjoint equation for $n = N, N-1, \ldots, N-B+1$ using the state equation solution for $n = N-B+1, N-B+2, \ldots, N$ and compute the gradient of the performance function.
6. Solve the state equation and store the solution for $n = (A-2)B+1, (A-2)B+2, \ldots, (A-1)B-1$.
7. Solve the adjoint equation for $n = (A-1)B-1, (A-1)B-2, \ldots, (A-2)B+1$ using the solution of the state equation for $n = (A-2)B+1, (A-2)B+2, \ldots, (A-1)B-1$ and compute the gradient of the performance function.
8. Set $A = A-1$ and go to step 6.

The number of storage requirements is $A + B$. Thus, to minimize the storage, $A + B$ needs to be minimized. If $N^{1/2}$ is an integer, the minimum is attained for $A = B = N^{1/2}$. Therefore, the storage requirement is $2N^{1/2}$ instead of N.

The efficiency of TDDM is validated for the numerical example (Section 5.2). In this example, the number of time steps is set at 2500. The relation between the divided section A, the time step B in the divided section, EXE size and reduction ratio is given in Table I.

If the divided section A is equal to the time step B in the divided section, the computational storage requirements can be minimized. Applying the TDDM to this example, the computational storage requirements can be reduced by 81.4%.

For large-scale optimization problems, this method increases the efficiency of practical computation.

5. NUMERICAL EXAMPLE

5.1. Control problem of water level for multiple conduits

5.1.1. Computational model. For the control problem of water level, the multi-conduits problem is adopted. In this study, 'flood control system (I)' shown in Figure 1 is applied. It is assumed that there are four main conduits connected with six bypass conduits. The computational model is illustrated in Figure 5. The main conduits is 100 m and that of the bypass conduits is 5 m.

Inflow boundary conditions for each main conduit are shown in Figure 6. It is assumed that one peak discharge occurs for the conduits A and D. Steady discharge is applied to conduits B and C. The initial condition of the water level is defined as shown in Figure 7. It is established that the water levels in the main conduits B and C are lower than those of main conduits A and D. Therefore, if a large volume of water is injected to main conduits A and D, the water level of main conduits A and D can be maintained at the target water level by diversion to main conduits B and C.

Therefore, the target points are set at the centre of main conduits A and D. Here, the purpose is to find the optimal control discharge for reducing the water level of main conduits A and D to the target water level.

Table I. Relation of between A, B, EXE size and reduction ratio.

A	B	EXE size (MB)	Reduction ratio (%)
1	2500	1844	0.0
2	1250	1075	41.7
5	500	614	66.7
10	250	346	81.2
50	50	343	81.4

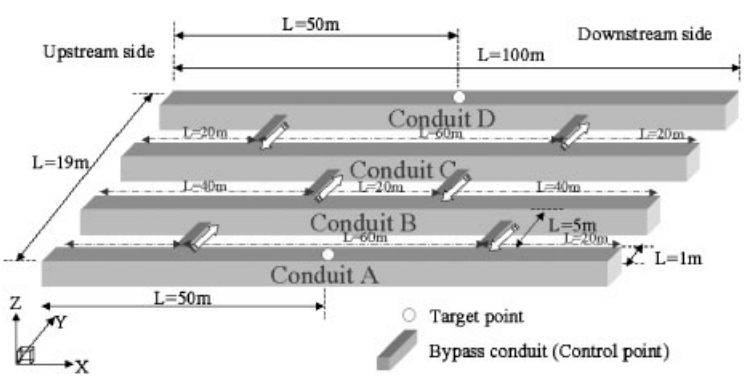

Figure 5. Computational model.

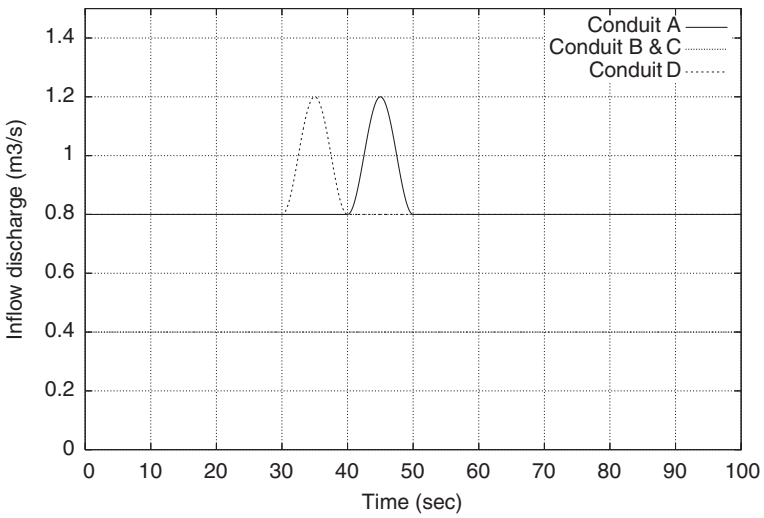

Figure 6. Inflow boundary condition.

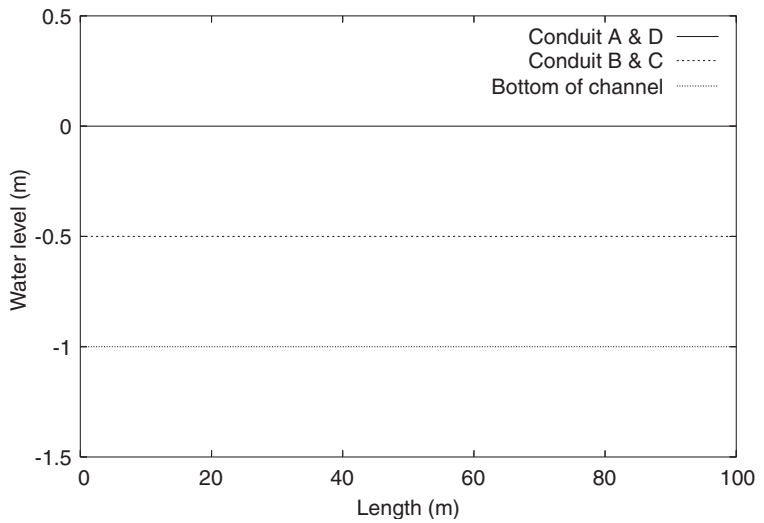

Figure 7. Initial condition of water level.

5.1.2. Treatment of control boundary and finite element mesh. To treat this type of control problem, the following two items need to be considered:

- The water level becomes discontinuous between the main conduit and bypass conduit. Therefore, the conduits cannot be connected by a finite element mesh.

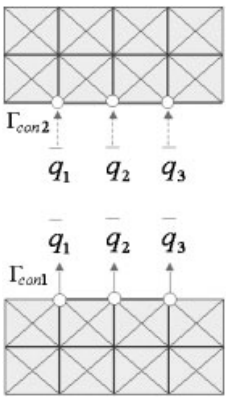

Figure 8. Treatment of control boundary.

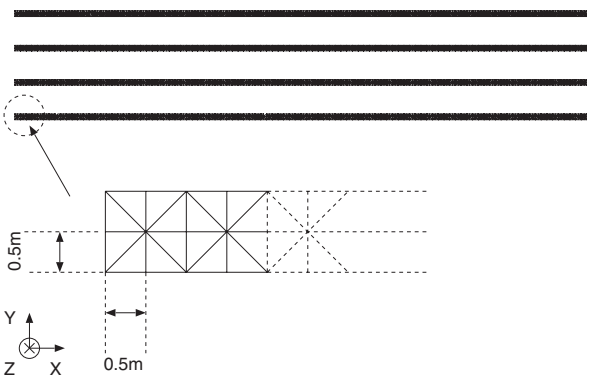

Figure 9. Finite element mesh.

- As a result of diversion by the control device, the inner bypass conduit fills to the ceiling and is subjected to pressure. Consequently, the assumption of shallow-water flow is not realized.

Based on these facts, the finite element mesh of the bypass conduit is not generated to avoid the discontinuous of water surface between the bypass conduit and the main conduit, and to satisfy the assumption of the shallow-water flow. It can be treated that the control discharge on Γ_{con1} is same as the control discharge on Γ_{con2}, because the inner of the bypass conduit is the state of pressure. Therefore, the computed control boundary condition on Γ_{con1} is given on the Γ_{con2} as shown in Figure 8. Hence, the finite element mesh shown in Figure 9 is used in this study, and consists of main conduits only. The total number of nodes and elements are respectively, 2520 and 3320.

5.1.3. Computational condition and numerical results. The purpose of this study is to determine the optimal control discharge for each bypass conduit to approach the computed water level to the target water level at the target points.

Table II. Computational condition.

Number of time steps	2500
Time increment, Δt (s)	0.04
Kalman constant, κ_l	0.41
Manning coefficient of roughness, n (s/m$^{1/3}$)	0.013
Weighting constant, Q	1.0
Weighting constant, R	0.0001
Weighting constant, W	0.2
Target water level, η_{Target} (m)	−0.10

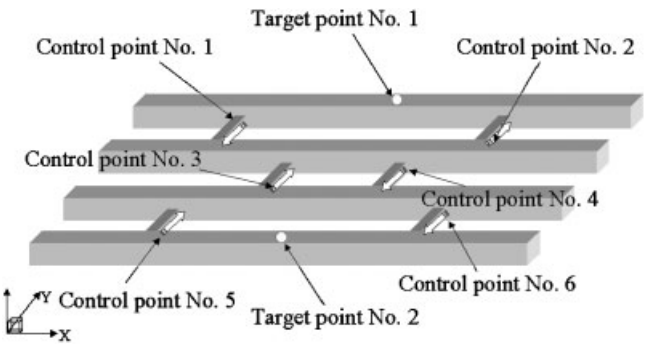

Figure 10. Number of control points and target points.

The computational conditions for this analysis are listed in Table II. The weighting constant Q at the target point is 1.0 and at other points is 0.0. The weighting constant R at the control point is 0.0001 and at other points are 0.0. The weighting constant W at the target point is 0.2 and at other points are 0.0.

The number of control and target points is shown in Figure 10. The direction of the injection of control discharge is determined as being in one direction, since the control device, a pump, cannot suck water: it only discharges water. The computational results are shown in Figures 11–15. Figure 11 shows the variation in the performance function. It can be seen that the performance function decreases and converges. This means that the computed water level with optimal control is as close as the target water level. Consequently, the time history of the control discharge, shown in Figures 12 and 13, can be obtained. It can be found that the control devices do not work at Nos. 2, 3, 4 and 6. The reason, in this numerical model, is the target points were set only at conduits A and D, making it unnecessary to inject from conduits B and C to conduits A and D. These numerical results are thus entirely expected. Furthermore, the response of control discharge for point Nos. 1 and 5 is marked. In this numerical example, one periodic wave is given on the left side of conduit A and D. In Figures 14 and 15, it is seen that one peak water level occurs in cases without control. Similarly, in Figures 12 and 13, the response of control discharge for the response of peak water level without control can be seen. Hence, it is clear that appropriate control discharge can be obtained by using the optimal control theory. Figures 14 and 15 show the time histories of water level at target point Nos. 1 and 2. The solid line indicates the non-control case and the broken line indicates

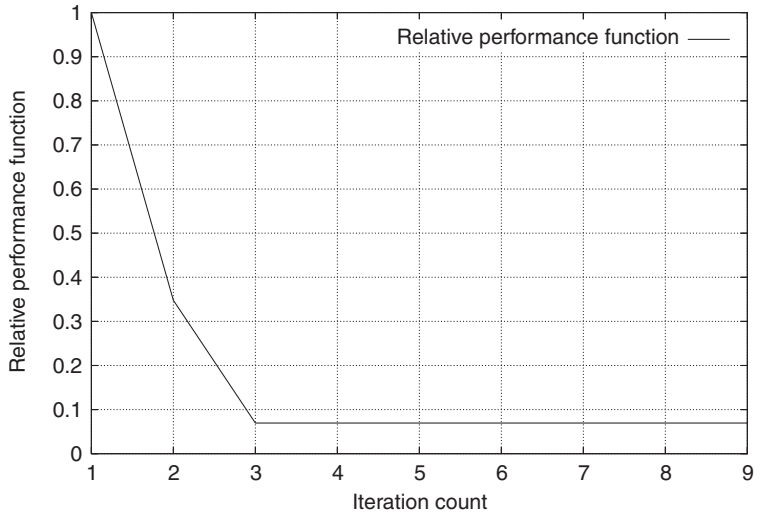

Figure 11. Variation in performance function.

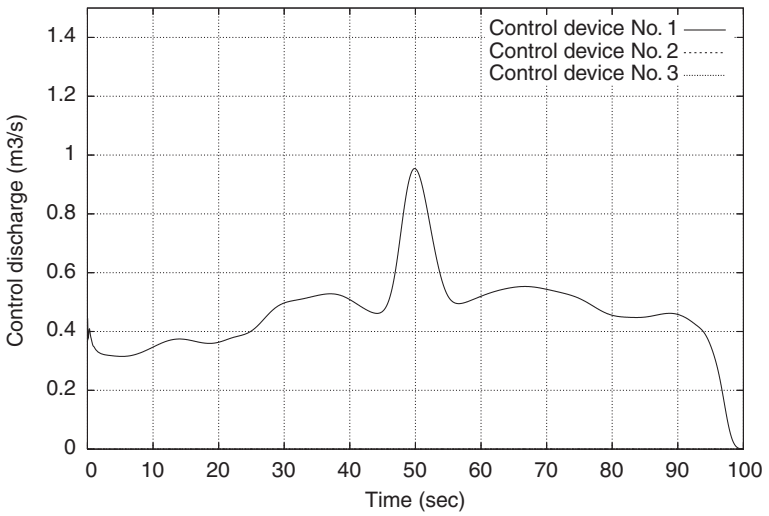

Figure 12. Time history of control discharge at control point Nos. 1–3.

the optimal-control case. The target water level was set -0.10 m. At both target points, the water level could be made to the target water level.

5.1.4. Remarks for terminal condition of Lagrange multiplier. In this paper, a method is proposed for determining the terminal condition of the Lagrange multiplier. Conventionally, the terminal condition of the Lagrange multiplier has been treated as zero in all iteration cycles,

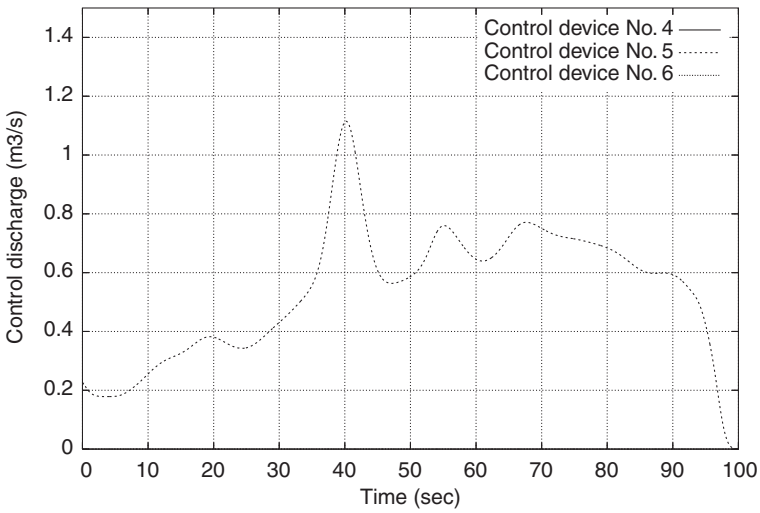

Figure 13. Time history of control discharge at control point Nos. 4–6.

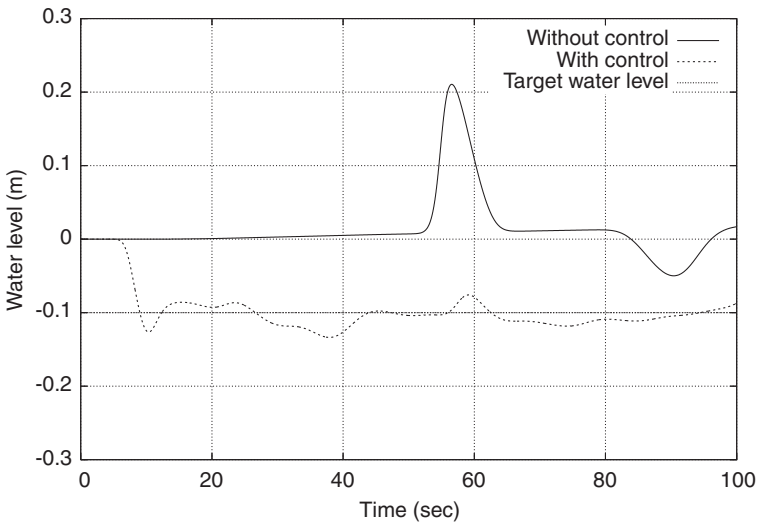

Figure 14. Time history of water level at target point No. 1.

and as a result, the control value near the terminal time has not been adequately expressed. To settle this problem, a method for determining the terminal condition of the Lagrange multiplier via a solution using a steady adjoint equation is proposed. The influence of terminal condition of Lagrange multiplier was investigated using the computational results for control discharge between the present and conventional methods. Figures 16 and 17 show a comparison of the control discharge at control point Nos. 1 and 5 between the present and the conventional

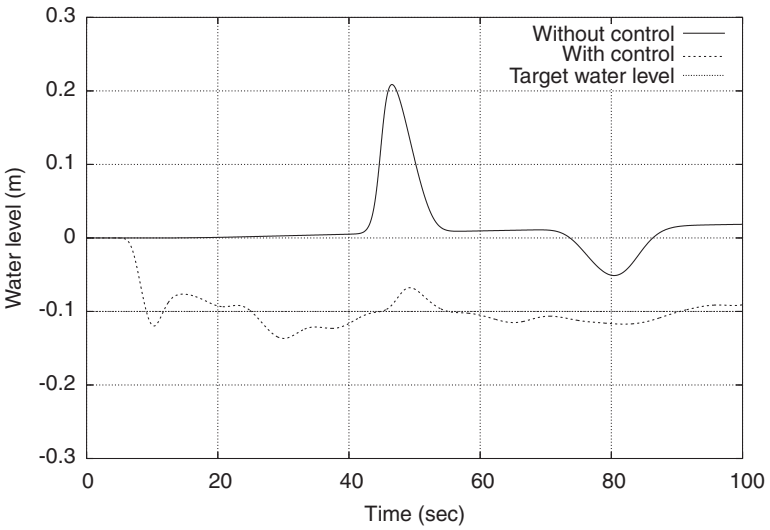

Figure 15. Time history of water level at target point No. 2.

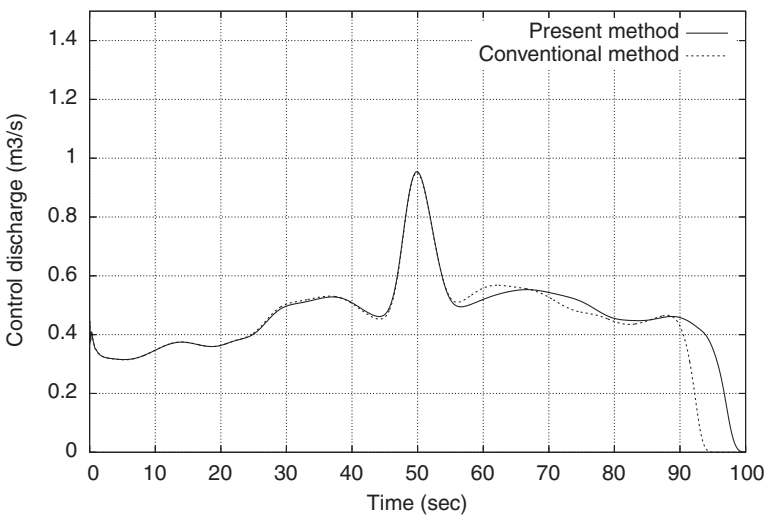

Figure 16. Comparison of control discharge at control point No. 1 between present method and conventional method.

methods. In the conventional method, in which the terminal condition of the Lagrange multipliers is set at zero, the control discharge near the terminal time gradually falls to zero under the influence of the terminal condition. However, in the present method, the control discharge near the terminal time can be improved over that obtained by the conventional method. Moreover, the distribution of the Lagrange multiplier at the terminal time is investigated. The distribution of Lagrange multipliers for each state variable are shown in Figures 18 and 19. Figures 18 and

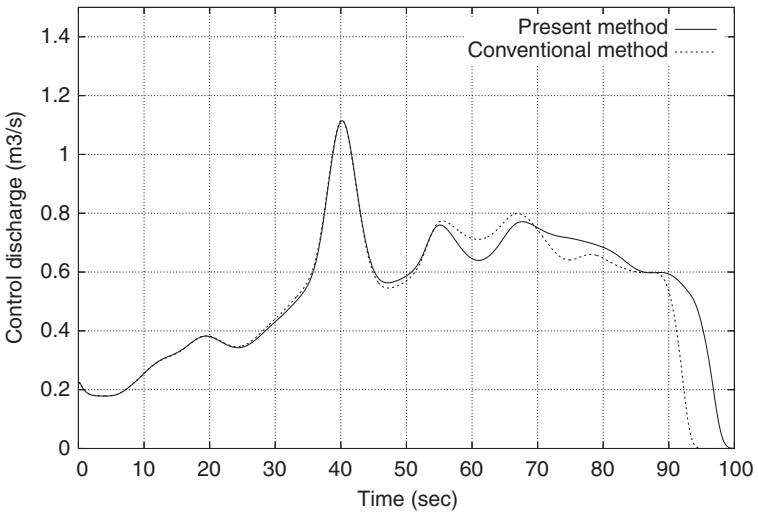

Figure 17. Comparison of control discharge at control point No. 5 between present method and conventional method.

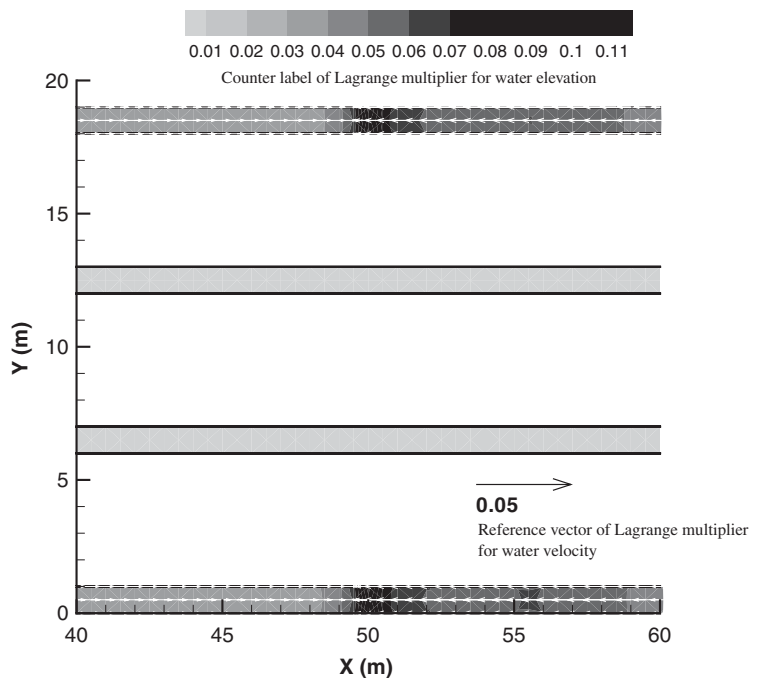

Figure 18. Distribution of Lagrange multipliers at first iteration.

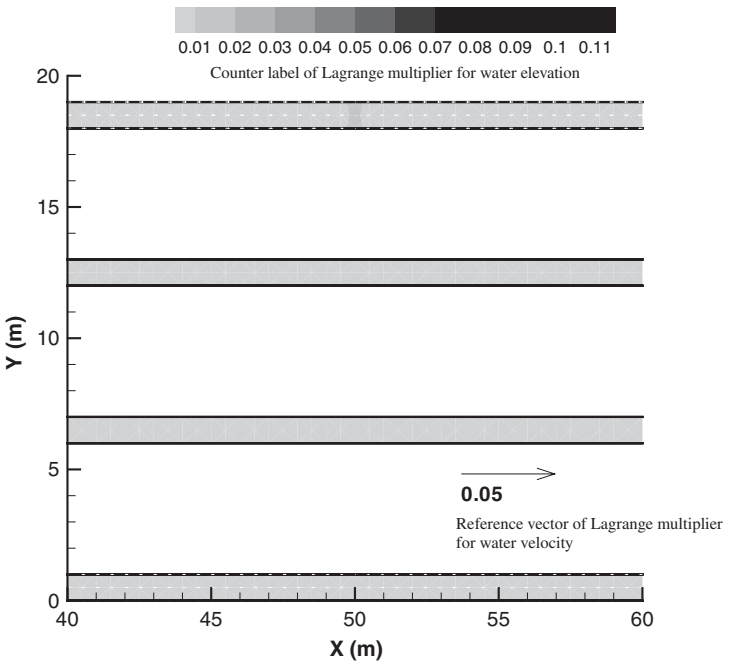

Figure 19. Distribution of Lagrange multipliers at final iteration.

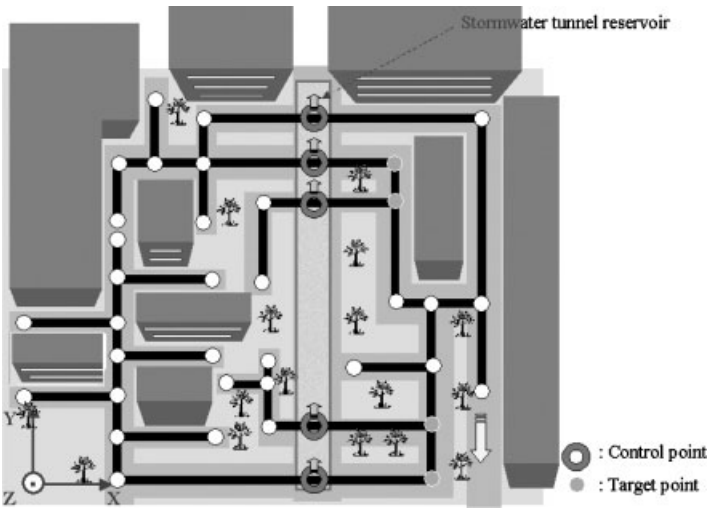

Figure 20. Computational model.

19 denote the distribution of the Lagrange multipliers at the first and final iteration. In Figure 18, the distribution of Lagrange multipliers can be confirmed: they finally converge to zero, as shown in Figure 19. This means that the first variation of extended performance function is satisfied.

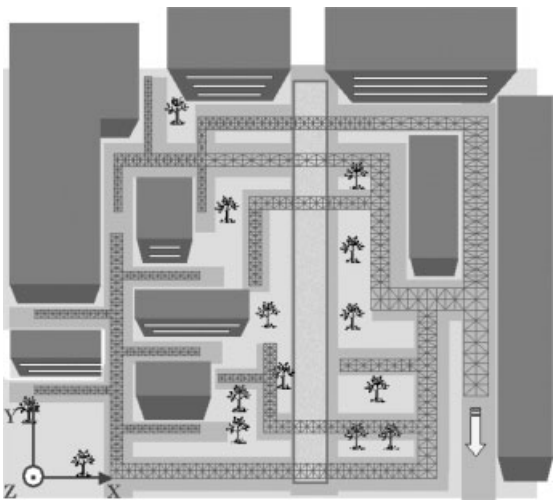

Figure 21. Finite element mesh.

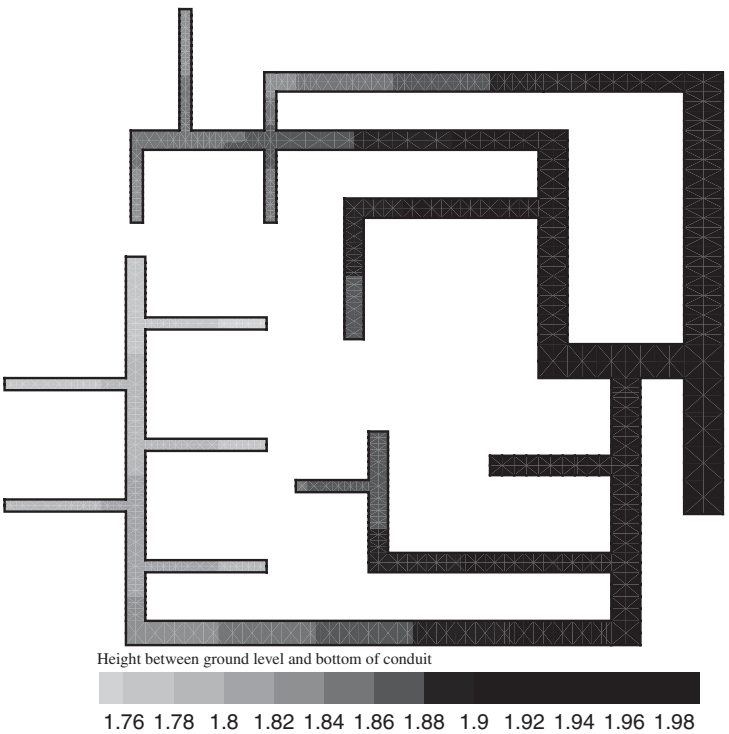

Figure 22. Height between ground level and bottom of conduit.

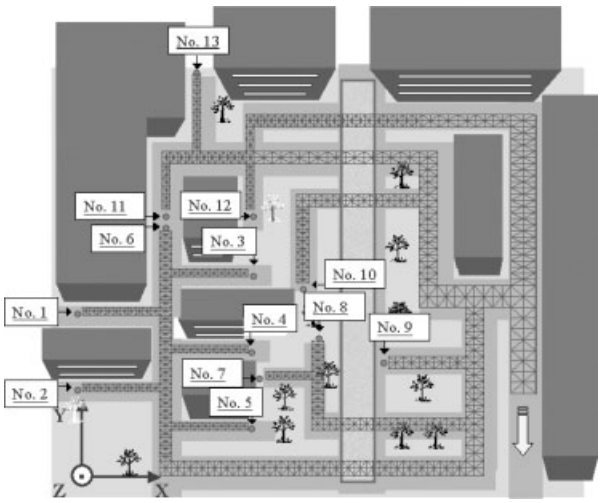

Figure 23. Number of inflow points.

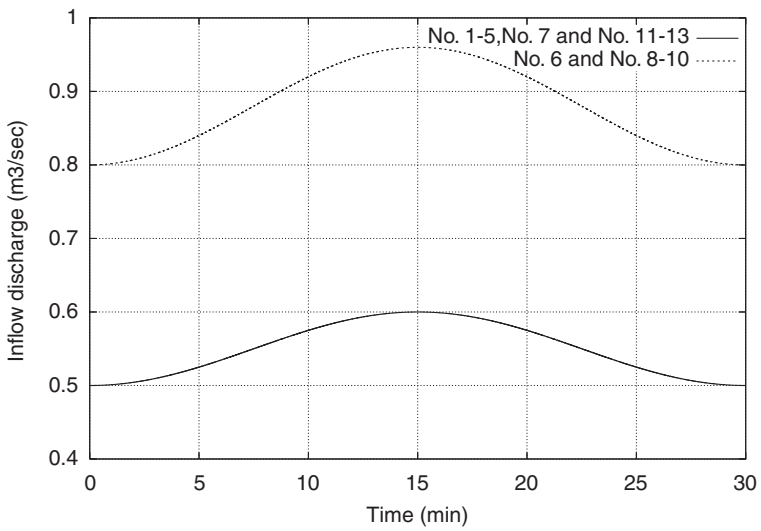

Figure 24. Time history of inflow discharge on inlet boundary.

5.2. *Control problem of water level for complicated network of conduits*

5.2.1. Computational model and computational conditions. In this section, a complicated network of conduits is used as a numerical study. The computational model is illustrated in Figure 20. In this study, 'flooding control system (II)', shown in Figure 2 is applied. Since the adequate control discharge needed to reduce the water level cannot easily be obtained at each control point, a complicated network is employed. Therefore, we examine here whether adequate control discharge can be achieved by using optimal control theory. This control

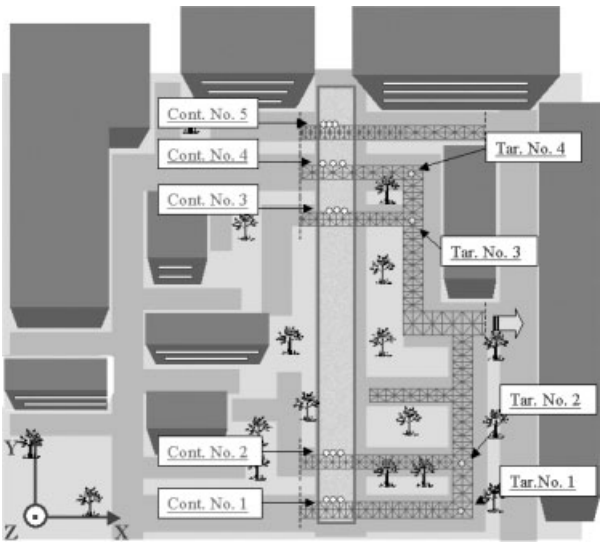

Figure 25. Target points and control points.

Table III. Computational condition.

Number of time steps	18 000
Time increment, Δt (s)	0.1
Kalman constant, κ_l	0.41
Manning coefficient of roughness, n (s/m$^{1/3}$)	0.013
Weighting constant, Q	1.0
Weighting constant, R	0.0001
Weighting constant, W	0.9
Target water level, η_{Target} (m)	0.0

system is based on the assumption that the water levels at the target points can be controlled by injecting water from the control points to the stormwater tunnel reservoir. The finite element mesh and height between ground level and the bottom of the conduit are shown in Figures 21 and 22. The total number of nodes and elements are 1665 and 2220, respectively. It is assumed that the ground water level is flat; height, therefore, means the elevation of the bottom of the conduit from the flat ground surface. The number of inflow points are illustrated in Figure 23. There are two types of width at the inflow points. The width of conduits is 0.5 m at inflow point Nos. 1–5, 7 and 11–13; and 0.8 m at inflow point Nos. 6 and 8–11. The inflow discharge at each point is shown in Figure 24. Here, the four target points and five control points are set as shown in Figure 25. The purpose of this study is to obtain the control discharge at each control points that makes the computed water levels approach the target water level as closely as possible.

The computational conditions for this analysis are displayed in Table III. The weighting constant Q at the target point is 1.0 and is 0.0 at other points. The weighting constant R at

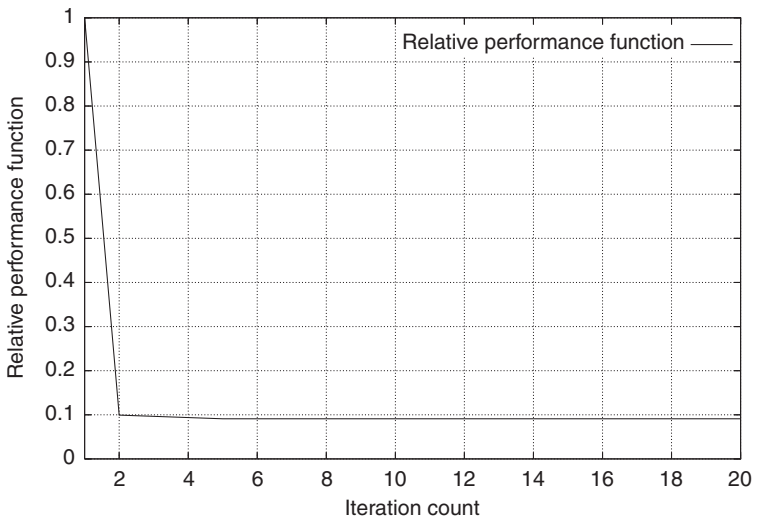

Figure 26. Variation in performance function.

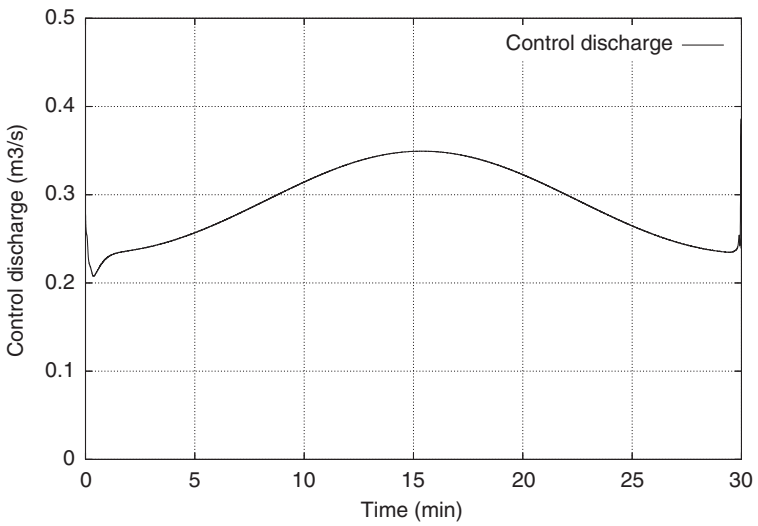

Figure 27. Time History of control discharge at control point No. 1.

the target point is 0.0001 and is 0.0 at other points. The weighting constant W at the target point is 0.2 and is 0.0 at other points.

5.2.2. Numerical results. Firstly, the variation of the performance function is shown in Figure 26. Consequently, the value of the performance function can be reduced by 90.9%. Secondly, the time history of control discharge is shown in Figures 27–31. The variations in the control discharge are similar to the variations of the inflow discharge. Adequate con-

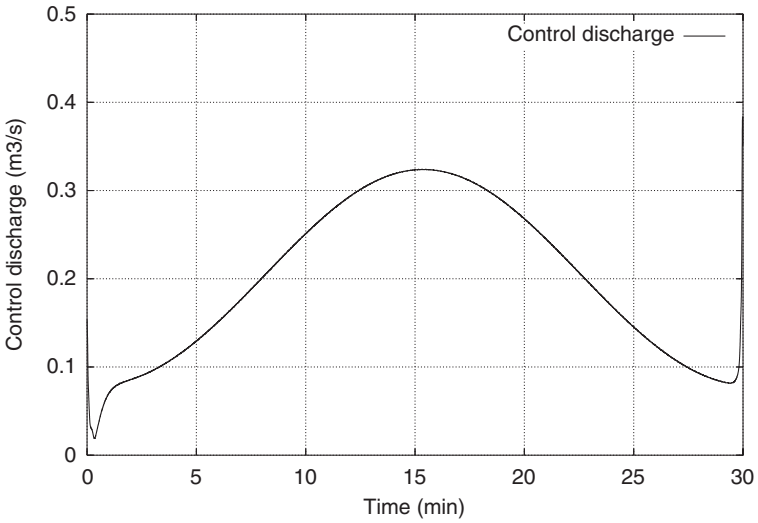

Figure 28. Time history of control discharge at control point No. 2.

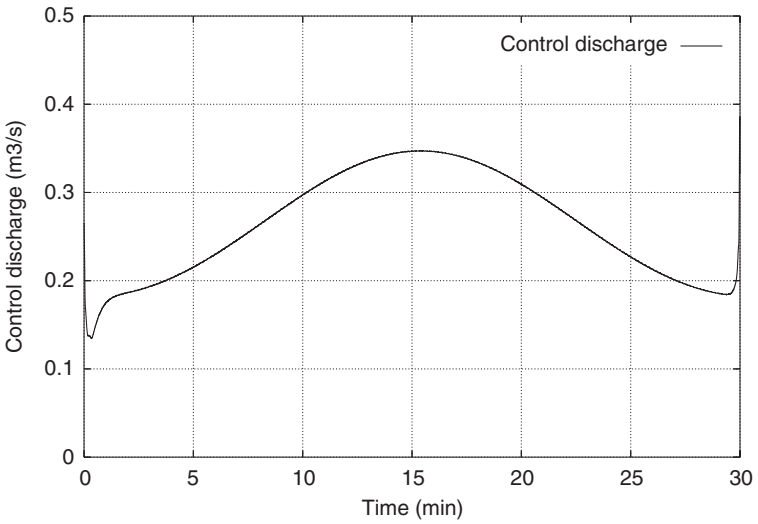

Figure 29. Time history of control discharge at control point No. 3.

trol discharges can be numerically obtained using optimal control theory. Thirdly, the time history of the water level at the target points from Nos. 1 to 4 are shown in Figures 32–35. At the target point Nos. 1 and 2, the water level did not reach close enough to the target value, possibly due to convergence at a local minimum point. However, the water level was successfully reduced to the target water level at target point Nos. 3 and 4.

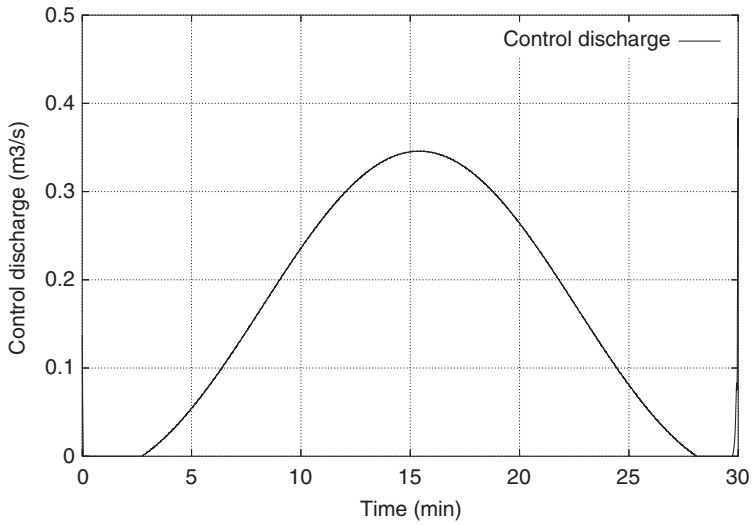

Figure 30. Time history of control discharge at control point No. 4.

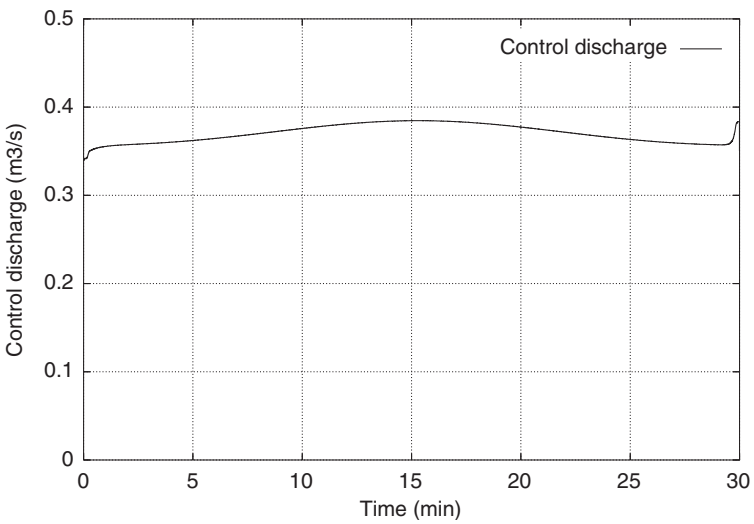

Figure 31. Time history of control discharge at control point No. 5.

6. CONCLUSIONS

In this paper, optimal control theory was employed to calculate the optimal control discharge needed to reduce the water level at the target points. As state equations, the shallow-water equation was employed to express water behaviour. The Galerkin method using the bubble function element with stabilized operator control term [5, 6] which is derived using the SUPG

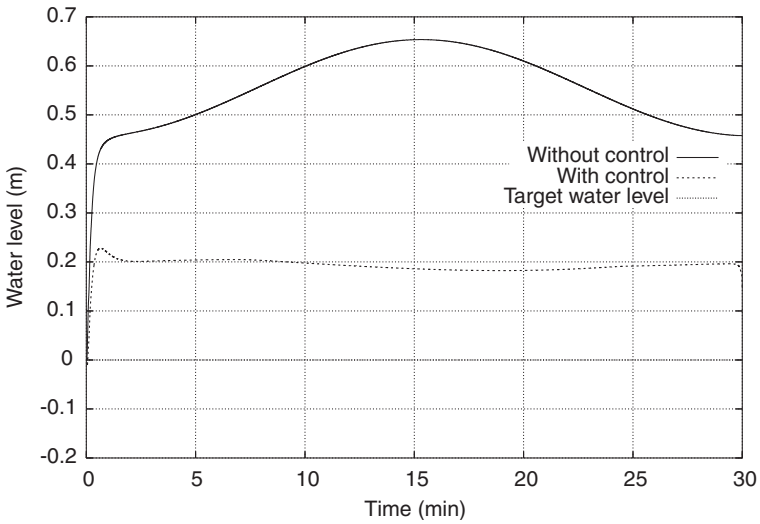

Figure 32. Time history of water level at target point No. 1.

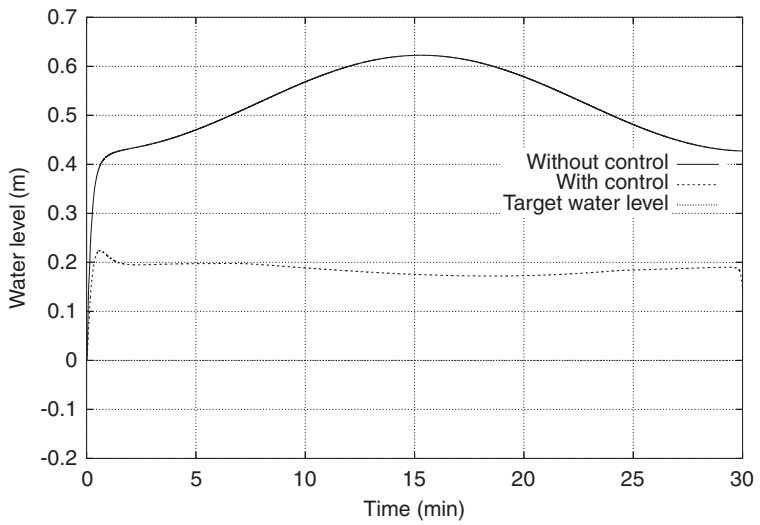

Figure 33. Time history of water level at target point No. 2.

method [7] and the Crank–Nicolson method, respectively, were used for the spatial and temporal discretizations. The Sakawa–Shindo method was used as the minimization technique [8]. A method was also presented for determining the terminal condition with respect to Lagrange multiplier. As the numerical examples, the following problems were used:

1. Control problem of water level in multiple conduits.
2. Control problem of water level in complicated network of conduits.

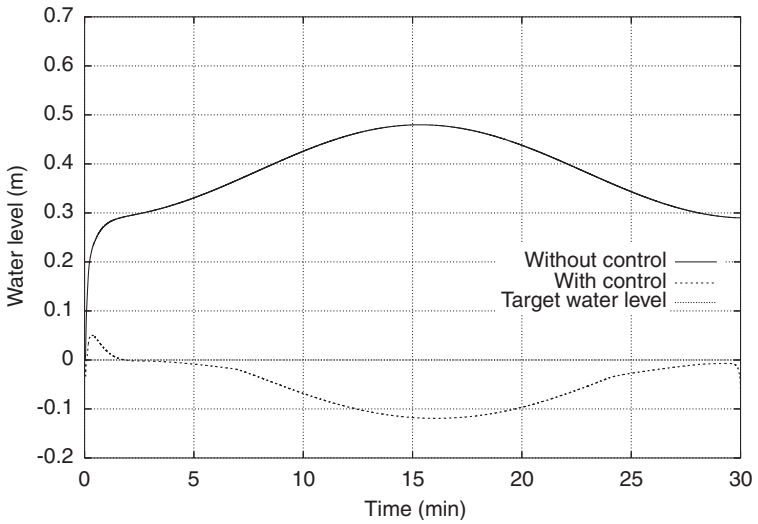

Figure 34. Time history of water level at target point No. 3.

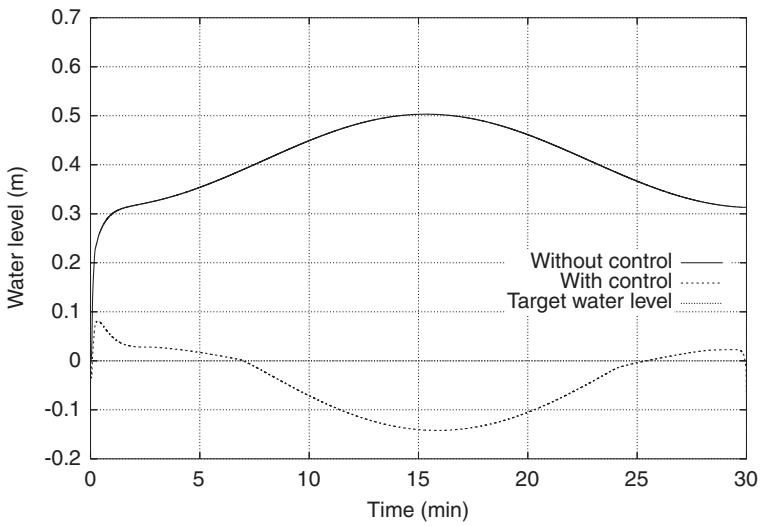

Figure 35. Time history of water level at target point No. 4.

The conclusions of this study are written as follows:

- Optimal control discharge can be obtained by using optimal control theory.
- Whether this approach is effective or not can be judged by whether or not a bypass conduit and control device are required.
- The control discharge can be estimated before the construction of this type of control system.

- The water level in the surcharge conduit can be reduced to the target water level by constructing bypass conduits and control devices.
- The proposed method for determining terminal conditions with respect to the Lagrange multiplier is useful for evaluating adequate control values near the terminal time.

Those conclusions suggest that it is necessary to apply this control theory to flood-limiting designs. The size of pumps and the height of side weir can be appropriately determined using the results of analysis carried out on the initial design.

Furthermore, the time domain decomposition method was applied to this problem [9, 10]. As a result, the computational storage requirements could be drastically reduced. However, this method has a drawback in terms of computational time, since the state equation has to be calculated twice per iteration. Hence, a great deal of computational time is required to obtain an optimal solution. To counteract this disadvantage, high-performance minimization technique should be employed.

REFERENCES

1. Jameson A. Computational aerodynamics for aircraft design. *Science* 1989; **245**:361–371.
2. Jameson A, Pierce N, Martinelli L. Optimum aerodynamic design using the Navier–Stokes equation. *Theoretical and Computational Fluid Dynamics* 1998; **10**:213–237.
3. Nakagawa H, Nakagawa O. Studies on the flow behaviours over the side weirs. *Disaster Prevention Research Institute*, *Kyoto University*, *Annual Report* 1968; **11B**:1–17.
4. Kurahashi T, Kawahara M. Water quality control by bank placement based on optimal control and finite element method. *International Journal for Numerical Methods in Fluids* 2003; **41**:319–338.
5. Matsumoto J, Khan AA, Wang SSY, Kawahara M. Shallow water flow analysis with moving boundary technique using improved bubble element. *International Journal of Computational Fluid Dynamics* 2002; **16**(2):129–134.
6. Matsumoto J, Umetsu T, Kawahara M. Stabilized bubble function method for shallow water long wave equation. *International Journal of Computational Fluid Dynamics* 2003; **17**(4):319–325.
7. Tezduyar TE. Stabilized finite element formulations for incompressible flow computations. *Advances in applied mechanics* 1992; **28**:1–42.
8. Sakawa Y, Shindo Y. On global convergence of an algorithm for optimal control. *IEEE Transactions on Automatic Control* 1980; **AC-25**(6):1149–1153.
9. He JW, Glowinski R. Neumann control of unstable parabolic systems: numerical approach. *Journal of Optimization Theory and Applications* 1998; **96**:1–55.
10. Berggren M. Numerical solution of a flow-control problem: velocity reduction by dynamic boundary action. *SIAM Journal on Scientific Computing* 1998; **19**:829–860.

